DESIGN OF FLEXIBLE PIEZORESISTIVE SENSOR BASED ON CARBON BLACK-SILICON MATRIX COMPOSITE MATERIAL

Tianhao JING[1], Kexin XU[2], Xinhui SUI[3], Ronghao LI[4], Yulong CHEN[5]*, Yuhong YAN[6]

At present, characteristics such as high sensitivity, cycling stability, and fast response remain the pursuit of high-performance flexible piezoresistive sensors. However, due to the limitations of the mechanical properties of the material itself, it is difficult to significantly improve the sensing performance by simply changing the material type. In recent years, the use of innovative structural designs and composite conductive materials has been the mainstream direction of sensor development. This paper proposes to design a flexible piezoresistive sensor based on carbon black-silicon-based composites for detecting seed seeding quality in soil. Through theoretical calculations and software simulations, the optimal structure and material ratio were obtained, which could improve the performance of the sensor while minimizing the cost of production and manufacturing. The results show that the optimized design of the flexible piezoresistive sensor has high sensitivity, good cycling stability and agile response speed in the 0~5 N environment range, with a working accuracy of over 97%, demonstrating its superior detection performance.

Keywords: Flexible piezoresistive sensor; COMSOL simulation; Composite material; Seed detection

1. Introduction

In recent years, with the rapid development of the economy, pressure sensors have also been deeply integrated into various frontier fields and have found extensive applications [1-3]. Compared with traditional rigid sensors, flexible pressure sensors have the advantage of a higher fit to the object being measured and

[1] College of Agricultural Engineering and Food Science, Shandong University of Technology Zibo, 255000, China, e-mail: 2373843860@qq.com
[2]College of Agricultural Engineering and Food Science, Institute of Modern Agricultural Equipment, Shandong University of Technology Zibo, 255000, China, e-mail: 2536570601@qq.com
[3]Ainuo Instrument Co., Ltd. Qingdao, 266101, China, e-mail: 19862513127@163.com
[4]College of Agricultural Engineering and Food Science, Shandong University of Technology, Zibo, 255000, China, e-mail: 17658552256@163.com
[5*]College of Agricultural Engineering and Food Science, Institute of Modern Agricultural Equipment, Shandong University of Technology, Zibo, 255000, China, e-mail: cyl06471@sdut.edu.cn
[6]School of Information Engineering, Shandong Management University, Jinan, 250357, China, e-mail: Hongyu_yan@outlook.com

more flexible portability, and have now become the core of detection sensors [4]. Flexible pressure sensors can be classified into four types based on their sensing mechanisms: piezoresistive [5], piezoelectric [6], capacitive [7], and triboelectric [8]. These flexible sensors can convert external mechanical stimuli into electrical signals for output. Among them, piezoresistive sensors have developed rapidly due to their advantages such as simple fabrication process and relatively low cost, and have become one of the best-performing sensor types. Li Wei et al. [9] designed a highly sensitive piezoresistive sensor based on a braided structure, which has a high sensitivity response of 8.4 kPa^{-1} in the range of 8 kPa and a detection range of 100 kPa, and the response time is maintained between 250 and 750 ms under the action of a 20 g weight. And maintained a relatively stable performance over more than 2000 cycles, Huang et al. [10] designed a highly sensitive linear silicon-based piezoresistive pressure sensor and obtained sensitivity for circular diaphragms made of monocrystalline silicon, silicon carbide, and polycrystalline silicon with a thickness of 15 μm at a load pressure of 100 kPa. Through comparative analysis, it was demonstrated that the circular diaphragm had better sensitivity than the octagonal diaphragm. She et al. [11] fabricated a porous conductive flexible pressure sensor with excellent sensing performance by integrating warp knitted spacer fabric with conductive composite material, which had good sensitivity and linearity in the range of 0~160 kPa; With a response time of 140 ms and a recovery time of 166 ms at 10 kPa pressure, it can monitor human motion signals in real time. While flexible piezoresistive sensors have been evolving, there have been certain challenges in the design of their main structures, the optimization of conductive materials, and their integration with smart agriculture .

Therefore, this paper proposes to design a flexible piezoresistive sensor based on carbon black-silicon matrix composites, aiming to improve sensor performance to a certain extent while addressing some of the current problems in seeding detection and promoting the integration of flexible piezoresistive sensors with modern smart agriculture. The overall structure, size, shape, thickness and conductive layer material of the sensor were designed through theoretical calculations, finite element simulation in COMSOL software and material simulation in Digimat software to obtain the best solution, and finally the performance test was completed.

2 Working principle

The flexible piezoresistive sensor works mainly based on the piezoresistive effect of semiconductors. When the semiconductor material is

subjected to pressure or tension, its lattice structure deforms, resulting in a change in the band structure and a shift in the energy valley, which in turn causes changes in carrier mobility and concentration [13]. These changes affect electrical conductivity. Since resistivity is inversely proportional to electrical conductivity, it will also change accordingly.

According to Ohm's law, for a uniform square semiconductor material of length L, cross-section S, and resistivity ρ, the overall resistance value R can be expressed as:

$$R = \rho \frac{L}{S} \tag{1}$$

In a semiconductor, conductivity and resistivity are reciprocal to each other, that is:

$$\rho = \frac{1}{\sigma} \tag{2}$$

The electrical conductivity of a semiconductor is the sum of the contributions of electrons and holes to conducting electricity, which is expressed as:

$$\sigma = q(n\mu_n + p\mu_p) \tag{3}$$

Thus, the expression for resistivity can be written as:

$$\rho = \frac{1}{q(n\mu_n + p\mu_p)} \tag{4}$$

where q is the electron charge, n *is the* electron concentration, p *is the* hole concentration, μ_n is the electron mobility, μ_p is the hole mobility. Here, the carrier mobility μ can be expressed as:

$$\mu = \frac{q\bar{t}}{m^*} \tag{5}$$

where $\bar{t}$ is the mean free time of the carriers, m^* is the effective mass of the carriers.

When a semiconductor material is subjected to compression, the distortion within its lattice causes a change in atomic spacing, which in turn causes a change in carrier mobility, resulting in a change in the resistivity of the semiconductor material, as shown in Fig.1.

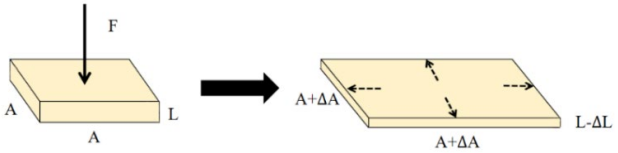

Fig.1 Piezoresistive effect of the schematic diagram

From this, it can be known that the flexible piezoresistive sensor can convert the perceived pressure signal into an electrical signal output. By taking advantage of this characteristic, such sensors can be used in the field of detection of seeds. The detection process is shown in Fig.2. The flexible piezoresistive sensor is installed at the bottom of the seed-pressing plate, and the seeds are identified by the pressure range and duration to detect the distribution of corn seeds in the soil during sowing and thereby determine the quality of sowing.

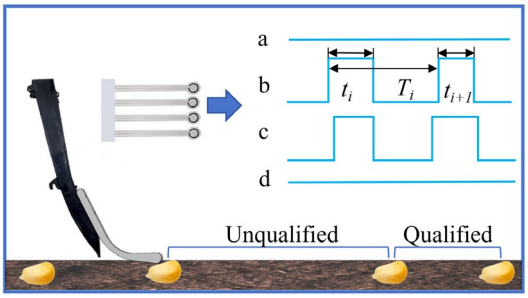

Fig.2 Schematic diagram of the flexible piezoresistive sensor for seed detection

3. Design and Experiment

3.1 Overall structure design of the sensor

The overall structure design of the sensor is based on the mainstream flexible sensor "sandwich" structure [14], and an optimized design is carried out on this basis. The specific structure is shown in Fig.3, and the base layer is composed of PE (protective film) and PDMS(polydimethylsiloxane) (substrate) superimposed. Due to the significant differences between the PE film and the conductive layer materials, it is difficult to bond them directly. Therefore, PDMS is used as an intermediary to ensure a good bond between the conductive layer and the base layer, and to reduce the interference of the external environment to the sensor. The electrode layer is made of metallic copper (Cu), whose main function is to conduct charges. The conductive layer is made of a composite of carbon black (CB) and silicon-based materials (including silicon sulfide, dimethyl silicone oil, tetraethyl silicate and dibutyltin dilaurate). Among them, the electrode layer forms a contact interface with the conductive layer, which is the core functional area for the flexible piezoresistive sensor to achieve piezoresistive effect.

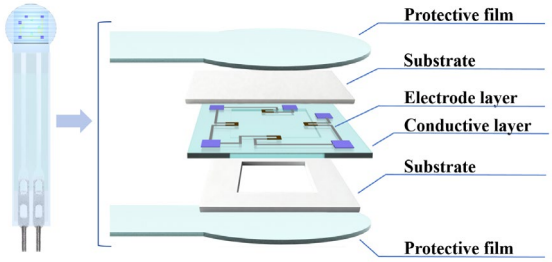

Fig.3 Schematic diagram of the sensor's layered structure

3.2 Key dimensions Design of the sensor

This study is used for seed identification during the seed pressing stage of corn sowing, by sensing the pressure signal of the seed in the soil trough and converting it into electrical signal feedback to determine the quality of sowing. So the sensor's sensing area should be able to fully cover the range of motion of the corn seed, and therefore the design of the sensor's key dimensions is particularly important.

3.2.1 Measurement of the size of the experimental subjects

To meet the design requirements, the triaxial dimensions of the corn seed need to be determined first to provide a basis for the sensor size design and the design of the detection algorithm.

This study selected Zhengdan 958 corn seeds as the experimental subject. This variety has strong adaptability and is widely distributed, making it a representative sample for testing. To ensure measurement accuracy, 100 seeds were randomly selected from the Zhengdan 958 corn seed sample. The length (L), width (W), and thickness (H) of each seed were measured using a vernier caliper as shown in Fig.4.

The average measurement results are presented in Table 1:

Table 1

The average dimensions of Zhengdan 958 corn seeds

Triaxial dimensions	Length (mm)	Width (mm)	Thickness (mm)
Average	11.86±0.66	8.92±0.52	4.77±0.44

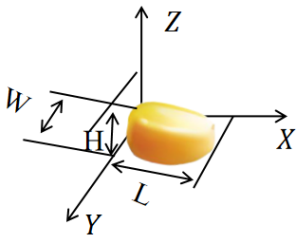

Fig.4 Method for Measuring the Three-Axis Dimensions of Seeds

The measurement results show that the average values of the three-axis dimensions of Zhengdan 958 corn seeds are 11.86 mm (L), 8.9 mm (W), and 4.77 mm (H) respectively, all close to the distribution peak. For the convenience of subsequent calculations, the final integer values L= 12 mm, W= 9 mm, H= 5 mm were taken as the three-axis dimensions of the seeds.

3.2.2 Design of sensor sensing area shape and size

In order to effectively distinguish seeds from soil, the shape and size of the sensor sensing area need to be determined through theoretical analysis and calculation as follows:

To ensure that the detection area can sensitively detect the seeds and facilitate calculation, this study first conducted a simulation analysis of the shape of the sensing area, comparing the square and circular design schemes.

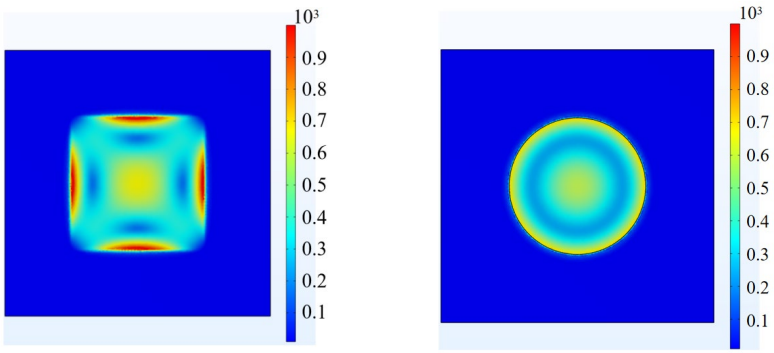

(a) Square area (b) Circular area

Fig.5 Simulation of the shape of the sensor sensing area

The simulation results are shown in Fig.5, indicating that the sensor sensitivity in the square sensing area is superior to that in the circular sensing area. As a result, the sensor's sensing area was eventually set to be square.

Set the width of the seed furrow area to 21 mm. Taking Zhengdan 958 corn seeds as an example, the lateral length range of the seeds is 9~12 mm (depending on the placement posture of the seeds).

The sensor must achieve full coverage of the seed furrow area. The side length a of the sensor film must satisfy the minimum value being equal to the width of the seed furrow area, that is:

$$a \leq 21 \text{ mm} \tag{6}$$

At the same time, in order to comprehensively detect the seeds within the area and distinguish between individual seeds and overlapping seeds, the length l of the sensing area needs to be greater than or equal to the maximum value of the lateral length of a single seed and less than or equal to the minimum value of the lateral length of an overlapping seed, that is:

$$12\ mm \leq l \leq 18\ mm \tag{7}$$

Based on the algorithmic determination rules, when the contact area between the sensing area and the seed is greater than 25% but less than or equal to 75%, it is determined as a single seed; when the contact area is greater than 90%, it is determined as an overlapping seed. Therefore, only when the edge length l of the sensing area is 14~17 mm can all situations be effectively detected. When l is 15 mm, the contact area between the sensing area and the single seed ranges from 36.0%~64.0%, which is in the middle section of the determination threshold, far away from the upper and lower limits. It has the strongest ability to resist seed placement deviations and sensor processing errors. Therefore, the final determination is that the sensor film has an edge length a of 21 mm, the sensing area has an edge length l of 15 mm, and the sensing area is located in the center of the sensor film.

3.2.3 Sensor thickness design

According to the mechanical properties of the square diaphragm, the maximum displacement at its center can be expressed as:

$$W_{max} = \frac{3PR^4}{16EH^3} * (1 - \mu^2) \tag{8}$$

where P is the pressure load (Pa), R is the edge length of the diaphragm (m), E and μ is the Young's modulus (Pa) and Poisson's ratio of the silicon membrane material respectively, H is the thickness of the diaphragm (m).

D is the bending stiffness of the diaphragm (N·m), which is expressed as:

$$D = \frac{EH^3}{12(1-\mu^2)} \tag{9}$$

To ensure good linearity of the sensor over the range, the diaphragm deformation must satisfy the small deflection theorem, requiring that the maximum deformation at the center of the diaphragm does not exceed 1/5 of the diaphragm

thickness, that is:

$$W_{max} = \frac{3PR^4}{16EH^3} * (1 - \mu^2) \leq 0.2H \tag{10}$$

The calculation results show that the sensor thickness H should satisfy H≥91.08 μm.

To determine the upper limit of the sensor thickness, stress simulation analysis of sensor films of different thicknesses (100 μm, 200 μm, 300 μm, 400 μm) was conducted using COMSOL simulation software. Since the substrate layer occupied the vast majority of the sensor thickness, the simulation was only conducted for the substrate structure. In the simulation, the pressure load was set to 10 Pa to observe the stress distribution of the sensor. The greater the stress tolerance, the higher the sensitivity and the better the performance of the sensor.

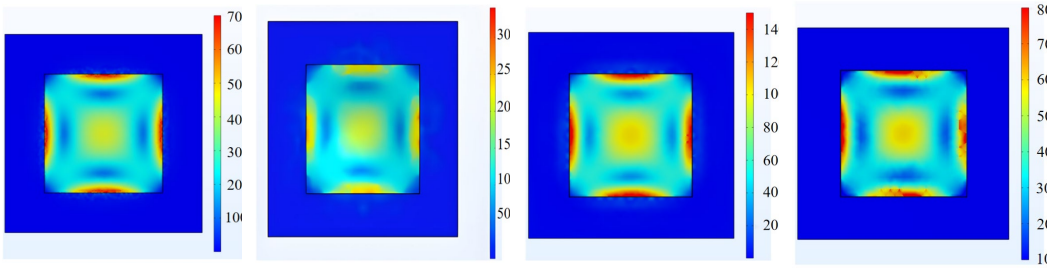

(a)100 μm (b)200 μm (c)300 μm (d)400 μm

Fig.6 Stress simulation of induction areas with different thicknesses

The simulation results are shown in Fig.6. It can be seen that as the thickness of the film increases, the stress that each part of the conductive layer can withstand gradually decreases. Therefore, the film thickness of the sensor should be as small as possible, so a thickness of 100 μm is taken.

Based on the structural design and material properties of the sensor, the thickness of each structural layer can be determined by the theoretical formula:

$$P_{max} = \frac{E \cdot t^3}{k \cdot L^4} \tag{11}$$

where E is the elastic modulus (Pa), t is the thickness (m), L is the characteristic length (the side length of the sensor film) (m), k is a constant, and for uniformly distributed square films, k is often taken as 1.27. The unit of the range P_{max} in the formula is Pascal (Pa), and it needs to be further multiplied by the sensing area of the sensor S (m²) to be converted into the actual Force (N), that is:

$$F = P_{max}S \tag{12}$$

Elastic modulus refers to the equivalent elastic modulus of the entire

sensor structure. Since the sensor is composed of multiple layers of material, the equivalent elastic modulus is needed to describe the overall mechanical properties, that is :

$$E_{eq} = \frac{\sum E_i \cdot t_i}{\sum t_i} \tag{13}$$

where E_i is the elastic modulus of the i-th layer (Pa), t_i is the thickness of the i-th layer (m). After calculation, the thickness of the PE film is 62 μm, the thickness of the PDMS is 22 μm, the thickness of the conductive layer is 2 μm, and the thickness of the electrode layer is 2 μm. This conforms to the thickness specifications of the nano-composite material film.

3.3 Sensor Conductive layer design and optimization

The conductive layer is the core component of the flexible piezoresistive sensor and directly determines the sensor's ability to sense pressure and convert signals. With the rapid development of flexible electronics technology, research on conductive layer materials has gradually shifted from traditional metal electrodes to composite materials with high flexibility and stretchability [15,16].

3.3.1 Material selection and working mechanism

The conductive layer is typically a composite material consisting of a matrix material and conductive fillers. The material selection and design of the conductive layer directly affect key performance of the sensor, such as sensitivity, linearity, response time, durability, and flexibility.

In this study, the base material of the conductive layer was prepared by mixing room temperature vulcanized silicone rubber, dimethyl silicone oil, tetraethyl silicate, dibutyltin dilaurate in a ratio of 40:4:2:1, and carbon black (CB) was used as the conductive filler. Among them, room-temperature vulcanized silicone rubber, as an ideal base material for flexible sensors, has excellent flexibility and stretchability; Dimethyl silicone oil and tetraethyl silicate act as plasticizers and crosslinkers to make the material blend more fully. Carbon black, as a conductive filler, can form a continuous conductive network in the silicone rubber matrix, giving the material good electrical conductivity.

The structure of the conductive layer was characterized using Digimat software, as shown in Fig.7. It can be seen that the conductive carbon black and the silicon-based material are in contact and entwined with each other in the composite, forming a complex but relatively uniform conductive network.

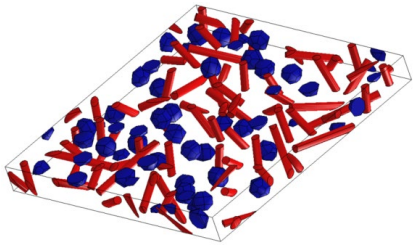

Fig.7 Characterization of the structure of the conductive layer mixture

The sensor conductive layer works as follows: when the sensor is not subjected to external force, the composite material of the conductive layer is looser and the carbon black particles are spaced far apart, resulting in lower conductivity and higher resistance. When the sensor is compressed by an external force, the gap between the carbon black and the silicon-based mixture decreases, the carbon black particle spacing shortens, the conductive network becomes denser, the conductivity increases significantly, and the resistance decreases.

3.3.2 Optimized design of the conductive layer material ratio

To ensure the performance of the sensor, this study obtained the optimal parameters of the conductive layer composite material ratio through simulation. The simulation process was based on COMSOL software, and the main procedures included model building, material property acquisition, physical field setting, parameter definition, meshing, and result calculation and analysis. The detailed description of the simulation is as follows:

(1) Model establishment and material property acquisition

This step is accomplished through the collaboration of Solidworks and Digimat software. In Solidworks, a three-dimensional model is created and then imported into the Digimat software for simulation. In the software, the basic properties and mixing ratio of the silicon-based matrix and carbon black filler are input, the collision determination conditions for particle no-crossing constraints and conductive contact threshold are set, the representative volume element (RVE) model is constructed and multi-scale simulation is solved to determine the material properties.

According to percolation theory [17], different conductive regions will be formed as the content of conductive fillers changes. In the initial stage, the content of conductive fillers is low, and no effective electron transfer path can be formed, making the material approach an insulator. As the content gradually increases, the conductive particles start to contact each other, and the resistance value of the composite material undergoes a sudden change. The content of conductive fillers at

this point is called the percolation threshold. If the content of conductive fillers is further increased, the resistance value will change suddenly again and tend to stabilize, and the material will approach a conductor. The content range between the insulator and the conductor is called the percolation range, and the piezoresistive characteristics presented within this range are obvious.

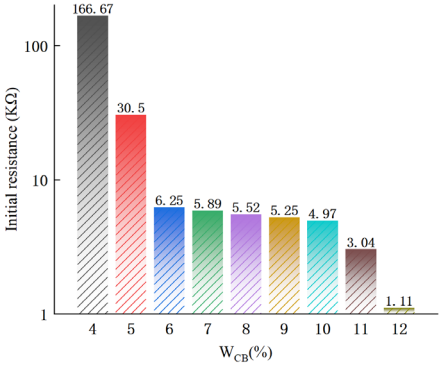

Fig.8 Initial resistance values of composites with different carbon black contents

The initial resistance magnitudes of composites with different carbon black contents can be obtained through material properties and simulation pre-experiments as shown in Fig.8. When the carbon black content is 4% to 6% (volume fraction, the same below), the resistance value changes abruptly and reaches the percolation threshold. When the carbon black content is further increased to 10% to 12%, the resistance value changes again. Thus, it can be determined that the percolation range of the composite material is approximately 4% to 12% carbon black content. Composite materials with carbon black contents of 4%, 6%, 8%, 10%, and 12% were selected for further simulation. This was done to systematically study the effects of different ratios on the performance of the sensors and to obtain their theoretical piezoresistive characteristic curves.

(2) Physical field Settings, parameter definitions and material selection

Two physical fields, the solid mechanics field and the current field, were set up in the simulation, and the piezoresistive effect was simulated through multi-physical field coupling.

① Solid mechanics field: used to simulate the deformation characteristics of the sensor under force. According to the Digimat simulation, the composite material is isotropic. A downward pressure of 0~5 N is applied to the upper boundary, and the lower boundary is fixed. The changes of the sensor under different pressures are studied.

② Current field: used to simulate the conductive properties of the sensor.

A fixed voltage is applied to one end of the sensor and the other end is grounded to form a conductive path and generate a distributed electric field. At the same time, the piezoresistive effect and domain current are set for multiphysical field coupling, causing the conductivity of the thin film material to change with pressure.

Globally define a pressure parameter to facilitate subsequent parametric scanning; At the same time, define an integral variable to integrate the normal plane of the flexible sensor for calculating the current I (plane integral × current density = current I).

Input all the material properties into COMSOL to simulate the stress distribution within the material. Set different materials according to different regions and assign various non-basic parameters to the materials, including electrical conductivity, relative dielectric constant, and piezoresistive coupling matrix, etc.

(3) Meshing

After setting the material property parameters, divide the mesh into "refinement" levels to ensure the accuracy of the calculation results. If the resistance value changes less than 2% with grid refinement, confirm that the current grid density has converged.

(4) Result calculation

The simulation model and calculation results are shown in the figure. The calculation object is the resistance value of the sensor.

During the simulation process, the current I varies with the pressure, while the voltage U remains constant. By calculating the change in resistance value with pressure, it is possible to intuitively analyze the variation pattern of sensor resistance and the influence of different mass ratios of composite materials on resistance variation.

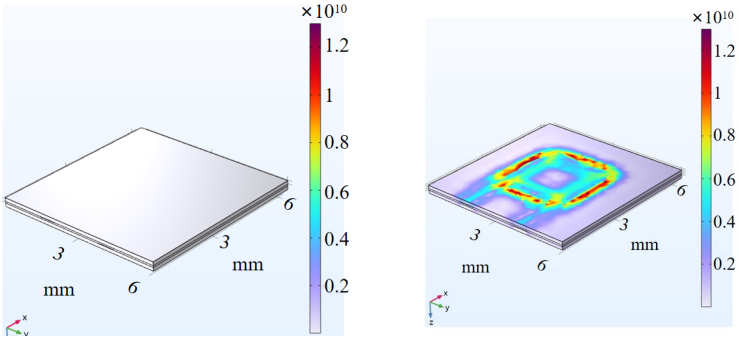

(a) Initial state (b) after pressure loading

Fig.9 Simulation of sensor stress under mean load

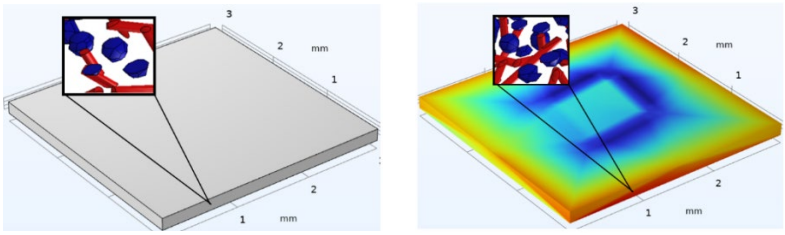

(a) initial state (b) after pressure loading

Fig.10 Distribution of conductive layer packing under mean load

The simulation process is shown in Figures 9 and 10. When the sensor film is subjected to external pressure, its cross-sectional area increases and its length decreases. The carbon black inside is in full contact with the silicon-based material to form a dense conductive path, which leads to a significant change in the internal resistance of the sensor, further verifying the piezoresistive characteristics of the material.

Based on the simulation results, the theoretical piezoresistive characteristic curves of five different carbon black content composite materials can be plotted as shown in Fig.11. It can be seen that the resistance value of the composite material decreases as the applied pressure increases. Within the 0~2 N pressure range, the resistance drops significantly. Beyond this pressure range, the change in resistance is relatively small compared to before, basically showing a linear trend, and gradually stabilizing.

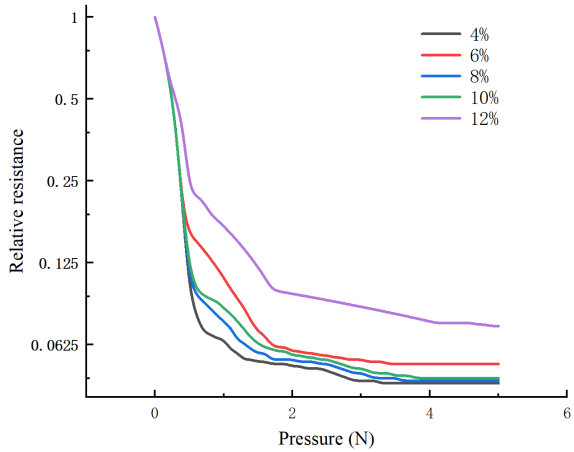

Fig.11 Theoretical piezoresistive characteristic curves of different carbon black contents

When the carbon black content is 4% and 8%, the resistance value of the composite material changes over a wide range and with high linearity as the pressure increases, but because the initial resistance value of the material with 4%

carbon black content is high, it is not conducive to the manifestation of piezoresistive effect at low voltages. Therefore, the 8% carbon black material was more in line with the actual requirements and expected results, so this study ultimately chose the 8% carbon black composite material as the conductive layer material for the sensor.

3.4 Sensor Preparation

The final processing and preparation of the sensor was carried out by Puhui Technology Company. Among them, the fabrication of the conductive layer was particularly crucial. Room-temperature vulcanized silicone rubber, dimethyl silicone oil, tetraethyl orthosilicate, and dibutyl tin dilaurate were mixed in a mass ratio of 40:4:2:1 using an electronic balance, and then evenly stirred with a magnetic stirrer to obtain the substrate. Subsequently, 8% (volume fraction) of conductive filler carbon black was added, resulting in a mixed solution. The composite material film was prepared by spraying process as the conductive layer. Finally, the various hierarchical structures were adhered together by adhesives to complete the encapsulation of the sensor.

3.5 Sensor performance testing

At present, characteristics such as high sensitivity, cycling stability, and fast response remain the pursuit of high-performance flexible piezoresistive sensors [18]. Therefore, the sensitivity, repeatability and response speed of the optimized sensors were tested separately, and soil trough experiments were conducted to verify their working performance.

3.5.1 Sensitivity test

In the actual detection process, changes in the contact area between the sensor and the object will affect the accuracy of the detection, and thereby influence the sensitivity of the sensor's detection. A pressure ranging from 0 N to 5 N was applied under different contact area conditions—specifically, at 100%, 75%, 50%, and 25% of the full contact area between the object and the sensor. The corresponding electrical response test curve was then plotted based on the recorded data.

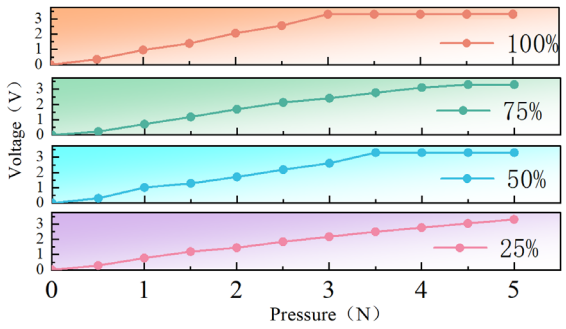

Fig.12 Electrical response test curves at different contact areas

From the test result Fig.12, it can be clearly seen that under the same force size, the voltage signals fed back by the sensors with different contact areas have the same overall change trend, all increasing with the increase in pressure. The curve of the 100% group has a relatively sharp upward slope, reaching the peak at 3 N; the curve of the 75% group has a slightly smaller slope than that of the 100% group, and the overall trend is more gentle; the curves of the 50% and 25% groups have an increasing slope in the later stage of the curve (greater than 2 N). Even if the contact area of the sensing area with the object is smaller than the total area of the sensing area, the sensor can still capture the subtle voltage differences caused by pressure changes and achieve effective signal response. This indicates that the sensor can maintain a stable high sensitivity under different contact areas and avoid the decrease in sensitivity caused by position movement, meeting the requirements of high-sensitivity sensors in practical scenarios.

3.5.2 Repeatability test

In the actual detection scenario, the sensor needs to perform the corn seed detection operation in a cyclic manner within the soil trough. The sensor needs to have excellent repeatability stability to ensure the accuracy of the final test results when the feedback signal remains stable after each pressing of the seed. The specific test process is as follows: An increasing pressure from 0 N to 3 N was applied to the sensor, after which the pressure was reduced from 3 N back to 0 N. This load–unload cycle was repeated more than 4,000 times in total. During the experiment, an STM32 microcontroller was used to collect the sensor output data in real time, and a signal curve graph was plotted based on the collected results.

From the test results shown in Fig.13, it can be seen that under the continuous action of cyclic pressure, the peak voltage of the sensor feedback has a low degree of dispersion, its standard deviation is maintained within a small range, and the differences of each peak voltage are also at a small level.

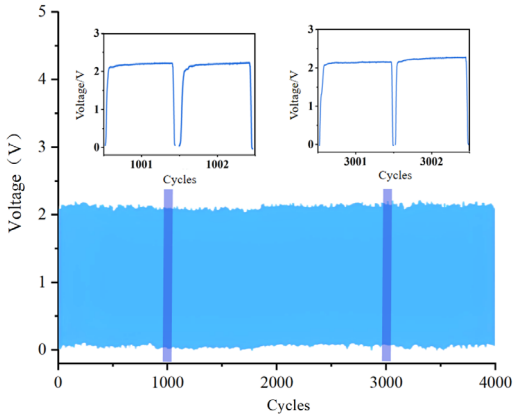

Fig.13 Repetitive stability test curve

In addition, in the repetitive cycle of pressure increase and decrease, the trend of voltage change corresponding to each pressure change shows a high degree of consistency. This result indicates that the sensor has excellent repeatability stability and can consistently output stable voltage signals during 4000 pressure loading-unloading cycles. The test results represent the lower limit of the sensor's stability lifespan. However, when actually detecting corn seeds, it is subjected to light loads and low impact contact, and the actual durability exceeds the test value by a significant margin. Moreover, the sensor's structural design is resistant to fatigue, allowing it to continuously complete corn seed detection without frequent replacements, thus meeting the practical application requirements.

3.5.3 Response speed test

The response speed of the sensor is the core indicator for evaluating its dynamic performance. Specifically, it refers to the time elapsed from when the sensor receives an external input signal until it outputs a measurement result that accurately reflects the signal and has stable values. During the repeated stability test of the sensor, the timer function of the single-chip microcomputer is utilized to capture its dynamic response characteristics. Through this function, the signal period can be collected in a high-frequency and high-precision manner in real time.

The sensor response test results are shown in Fig.14. The dynamic response performance of this sensor is excellent, with extremely fast response and recovery speeds: among them, the response time from receiving the signal to obtaining the stable measured value is only 16 ms, and the recovery time for the output value to return to the initial stable state is 21 ms.

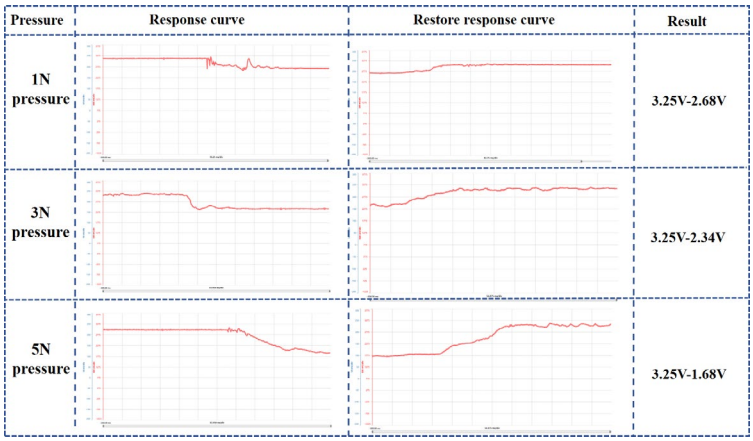

Fig.14 Sensor response curve

Taking the operation speed of the seed drill as 12 km·h^{-1} and the actual plant spacing as 0.15 m as an example, the corresponding seed interval time is approximately 45 ms, which is much greater than the response speed and recovery speed obtained from the test. This proves that the sensor can accurately complete signal capture and state restoration when passing through seeds continuously, meeting the rapid signal capture requirements for the normal operation speed of the seed drill.

3.5.3 Soil trough test

The soil trough test was conducted in an indoor soil trench laboratory, and the detection device is shown in Figure 15. A rectangular platform with dimensions of 1 m x 0.3 m x 1 m was built using industrial aluminum materials, and four tires with a diameter of 0.5m were installed on both sides. The STM32F103 series microcontroller was fixed above the seed-pressing plate, and then the sensor with the optimized design was installed at the bottom of the seed-pressing plate to complete the assembly of the cart. The cart was pushed forward at a certain speed, and during the process, the sensor conducted real-time detection of the corn seeds.

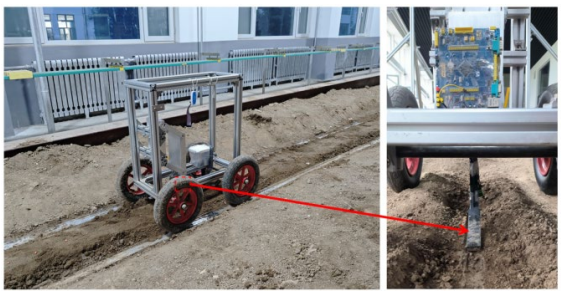

Fig.15 Soil trough test detection device

When the seed-pressing plate passes through the seeds in the soil trough, the sensor simultaneously identifies and detects them. Tests were conducted at speeds of 2~12 km·h^{-1}, repeated 10 times at each speed, with 150 corn seeds set for each group of tests.

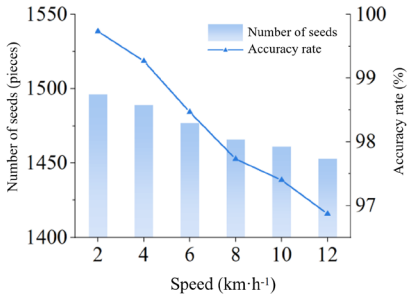

Fig.16 Results of the soil trough test

The results of the soil trough test are shown in Fig.16. It can be seen that when moving at a low speed (2~6 km·h^{-1}), the sensor performs well, and the average relative error detected is all less than 1.5%. When the speed increases to medium-high speed (8~12 km·h^{-1}), as the seed pressure frequency increases during the same period of time, the sensor may not be able to capture the pressure changes when some seeds pass through in time, resulting in seed omission, or due to the higher speed advance, some seeds do not fully contact the sensor, resulting in reduced detection efficiency. But the average relative error remains within 3 percent. Therefore, the optimized sensor can achieve an accuracy rate of over 97% when the seeding machine operates at its normal forward speed, meeting the actual working requirements.

4. Conclusions

(1) This paper designs a "sandwich" flexible piezoresistive sensor structure for seeding detection, consisting of a base layer (PE+PDMS), an electrode layer (Cu), and a conductive layer (composite material). Through theoretical calculation and simulation analysis, it was determined that the sensor film was a square with an edge length a of 21 mm, the sensing area was a square with an edge length l of 15 mm, and the sensing area was located in the center of the sensor film; At the same time, the thickness of the PE film is 62 μm, the thickness of the PDMS is 22 μm, the thickness of the electrode layer is 2 μm, the thickness of the conductive layer is 2 μm.

(2) Simulation analysis of parameters such as the ratio of conductive layer composites based on COMSOL and Digimat software. The results show that the

resistance value of the composite decreases with the increase of pressure applied. The resistance decreases significantly in the 0~2 pressure range. Beyond this pressure range, the resistance change is relatively small compared to before, basically linear, and gradually stabilizes. Composites with 8% carbon black content have a wider range of resistance values and higher linearity compared to other ratios, which are more in line with the actual requirements and expected results.

(3) Performance tests were conducted on the optimized flexible piezoresistive sensor, and the results showed: The sensor demonstrated high sensitivity, good repeatability stability (>4000 times), and agile response speed (within 21 ms) over a measurement range of 0~5 N, and an accuracy rate of over 97% in actual seed detection work, demonstrating the superior performance of the optimized sensor.

The flexible piezoresistive sensor based on carbon black-silicon matrix composites designed in this paper can improve sensor performance to a certain extent, promote the integration of flexible piezoresistive sensors with smart agriculture, and provide a reference direction for some of the problems currently faced in agricultural seeding detection.

Acknowledgments

This research was supported by the Key R&D Program of Shandong Province (Major Science and Technology Innovation Project) (Project No. 2025CXGC010807) and Shandong Province Agricultural Machinery R&D,Manufacturing,Promotion and ApplicationIntegration Pilot Proiect (Project No. NJYTHSD-202304).

REFERENCES

[1] *Wen Lei, Fan Wentian, Kang Jiahong*, et al. Porous pressure sensors from mechanisms to application: A review[J]. Sensors and Actuators A: Physical, 2025, 387: 116461.

[2] *Ghouila-Houri C, Talbi A, Viard R*, et al. High temperature gradient nanogap-Pirani micro-sensor with maximum sensitivity around atmospheric pressure[J]. Applied Physics Letters, 2018, 111(11):113502.

[3] *Muszynski MR, Olson SM*, Phillips C, et al. Earth Pressure Measurements Using Tactile Pressure Sensors in a Saturated Sand During Static and Dynamic Centrifuge Testing[J].Geotechnical testing journal, 2016.

[4] *Wang Ziyu, Liu Hongmei*, Ban Chuncheng. Fabrication and Characterization of Flexible Piezoelectric Films of Lead Magnesium Titanate and Lead Titanate (PMN-xPT) Based on Doped Graphene [J/OL]. Journal of Composite Materials, 1-8.

[5] *Zhao Yujian, Miao Luwei, Xiao Yao*, et al. Research progress of flexible piezoresistive pressure sensor: A review[J]. IEEE Sensors Journal, 2024, 24(20): 31624-31644.

[6] *Hadidi Sajad, Hassanzadeh Alireza*. A novel self-powered, high-sensitivity piezoelectric vibration sensor based on piezoelectric combo efect[J]. lEEE Sensors Journal.2023.23(21):25797-25803.

[7] *Mathew Soly, Chintagumpala Krishnamoorthi*. A review of recent progress in flexible capacitance pressure sensors: Materials design, printing methods, and applications[J]. Advanced Composites and Hybrid Materials, 2025, 8(3): 236.

[8] *Choi S B, Veeralingam S, Khanh T D*, et al. Rapid-response hybrid piezo-triboelectric pressure sensor using all-fabric materials for enhanced sensing and power generation[J]. Nano Energy, 2025:140.

[9] *Li Wei, Yao Wentao, Yang Bokai*, et al. Preparation and Performance of High-Sensitivity Piezoresistive Sensors Based on Weaving Structure Design [J/OL]. Chemical Industry Progress, 1-9.

[10] *Huang Yunzhi, Ma Shuai, Yin Zhongliang*, et al. Sensing Enhancement Design and Analysis of MEMS-Type Silicon-Based Piezoresistive Pressure Sensor [J/OL]. Rocket Propulsion, 2025, (04): 126-135 + 144

[11] *She Yemei, Peng Yangyang, Wang Fameng*, et al. Preparation and performance of flexible pressure sensor based on warp knitted spacer fabric[J]. Journal of Textile Research[J]. 2025, 46(03): 158-166.

[12] *Tian Yuyu, He Ren, Wu Juying*, et al. Performance Optimization Principles and Research Progress of Capacitive Flexible Pressure Sensors [J]. Materials Report, 2023, 37(16): 13-26.

[13] *He Qi*. Research on Temperature Compensation Method for Silicon Strain Gauge Pressure Sensor Based on PSO-ELM [J]. Measurement & Testing Technology, 2025, 51(09): 77-81.

[14] *Seesaard T, Wongchoosuk C*. Fabric-based piezoresistive Ti3AlC2/PEDOT:PSS force sensor for wearable E-textile applications[J]. Organic Electronics; Physics-Materials-Applications, 2023, 122(000):11.

[15] *Charara M, Luo W, Saha M C*, et al. Investigation of Lightweight and Flexible Carbon Nanofiber/Poly Dimethylsiloxane Nanocomposite Sponge for Piezoresistive Sensor Application[J]. Advanced Engineering Materials, 2019.

[16] *Zhang Yongfang, Wen Jingqian, Dong Lihong*, et al. Research Progress of Flexible Strain Sensors Based on Carbon Nanotubes and Their Composites [J]. Materials Report, 2024, 38(14): 70-80.

[17] *Shen Zhengpeng, Mei Qilin, Ding Guomin*, et al. Construction of Removable Salt-Assisted Graphene/Carbon Nanotube Network and Study on the Properties of Polyether Ether Ketone Composites [J/OL]. Composites Science and Engineering, 1-12.

[18] *Miao Yangyang, Chen Yongdang, Zhang Ya Jie*, et al. Flexible piezoresistive sensor based on silver powder-carbon nanotube-graphene composite sensitive material [J]. Light Industry Machinery, 2025, 43(02): 91-97 + 104.